Cerqueira Barros, S.; Alves Da Silva, A.; Costa, CM.; Lanceros-Mendez, S.; Barbosa Costa, D.; Tamano Maciavello, M.; Gómez Ribelles, JL.... (2015). Thermal-mechanical behaviour of chitosan-cellulose derivative thermoreversible hydrogel films. Cellulose. 22(3):1911-1929. doi:10.1007/s10570-015-0603-5.

THERMAL-MECHANICAL BEHAVIOR OF CHITOSAN-CELLULOSE DERIVATE THERMOREVERSIBLE HYDROGEL FILMS

Sandra Cerqueira Barros[1*], Ana Alves da Silva**[1], Diana Barbosa Costa**[1], Carlos M. Costa[2], Senentxu Lanceros-Mendez[2], M.N. Tamaño Machiavello[3], J. L. Gómez Ribelles[3,4], Franciani Sentanin[5], Agnieszka Pawlicka[5], Maria Manuela Silva[1]

[1] Centro de Química, Universidade do Minho, Campus de Gualtar, 4710-057 Braga, Portugal.

[2] Departamento/Centro de Física, Universidade do Minho, Campus de Gualtar, 4710-057 Braga, Portugal.

[3] Centro de Biomateriales e Ingeniería Tisular, Universitat Politècnica de València, 46022 Valencia, Spain

[4] CIBER en Bioingeniería, Biomaterials Y Nanomedicina, Valencia, Spain.

[5] Instituto de Química de São Carlos, Universidade de São Paulo, 13566-590 São Carlos, SP, Brazil.

* Corresponding author: Telephone: +351 253604370(86); Fax: +351 253604382; E-mail: xana@quimica.uminho.pt

** These authors contributed equally to this work.

Key words. Chitosan; (Hydroxypropyl)methyl cellulose; Thermal analysis; Rheological studies.

Abbreviations. CH, Chitosan; HPMC, (Hydroxypropyl)methyl cellulose; FT, Freeze-thaw; SC, Solvent casting; CH:HPMC (X:Y), pH Z, FT/SC, Chitosan and (hydroxypropyl)methyl cellulose hydrogel, at X and Y proportion (0-100), at Z pH (3.0-4.0) and prepared by freeze-thaw or solvent casting techniques; DSC, Differential scanning calorimetry; MDSC, Temperature modulated Differential scanning calorimetry; T_g, glass transition temperature; ΔH, enthalpy change; TGA, Thermogravimetric Analysis; TG, Thermogravimetry; DTG, Derivative or Differential thermogravimetry; σ, Tensile strength; ε, elongation at break; DMA, Dynamic mechanical analysis; X-Ray, X-radiation, FTIR-ATR, Attenuated total reflectance Fourier transform infrared spectroscopy; SEM, Scanning electron microscopy.

Abstract

Hydrogels are high water content materials prepared by polymer crosslinking that are able to release active species, such as therapeutic, antibacterial, antiperspirant and moisturising agents, and fragrances. In recent years, several hydrogel systems have been reported based on both natural and synthetic polymers. Among the natural polymers, chitosan and cellulose-derivatives have been extensively studied, due to their stimuli responsive properties (pH and temperature sensitivity, respectively). In this work, we have developed physically crosslinked hydrogel films based on chitosan (CH) and (hydroxypropyl)methyl cellulose (HPMC). These films were prepared by two methodologies: solvent casting (SC) and freeze-thaw (FT) techniques. The resulting membranes, were assessed in terms of thermal (DSC and TGA), mechanical (stress-strain mechanical assays and DMA) and structural (X-Ray) properties. The obtained results indicate that the developed CH:HPMC membranes show a good compatibility between the two component biopolymers. Additionally, these materials display an excellent thermal stability (having a $T_{Decomposition}$ > 270 ºC), good mechanical properties (especially for the compositions with similar contents of both polymers), a glass transition temperature (T_g) higher than 194 ºC and predominate amorphous character. The described characteristics turn the designed CH:HPMC membranes suitable candidates as active species carriers, for the envisaged textile application.

1. Introduction

Hydrogels are macromolecular networks able to absorb and release water solutions in a reversible manner (Sannino, Demitri & Madaghiele, 2009). The hydrogel structure is created by the hydrophilic groups or domains present in the polymeric network upon hydration in an aqueous environment (Zhang, Zhang & Wu, 2013). Polymer binding is accomplished either by non-covalent physical associations, such as molecular entanglements and secondary forces (including, hydrogen and ionic bonding or hydrophobic interactions) or by covalent crosslinking (Bhattarai, Gunn & Zhang, 2010; Gulrez, Al-Assaf & O Phillips, 2011; Hoffman, 2002). Physical associations are reversible bonds, whereas covalent crosslinking between polymer chains are not. Physical bonded hydrogels have the advantage of gel formation without the use of crosslinking entities (Bhattarai, Gunn & Zhang, 2010). Nevertheless, they also have limitations, such as weak/poor mechanical properties in the swollen state (Patel & Mequanint, 2011).

The water holding capacity, permeability along with the biocompatibility are the most important features of a hydrogel (Gulrez, Al-Assaf & O Phillips, 2011). The hydrogels biocompatibility is prompted by the high water content and the physiochemical (*i.e.*, compositional and mechanically) similarity of these materials with the native extracellular matrix (Hoare & Kohane, 2008). When a dry hydrogel begins to absorb water, the first water molecules entering the matrix will hydrate the most polar, hydrophilic groups, leading to *primary bound water* (Gulrez, Al-Assaf & O Phillips, 2011; Hoffman, 2002; Patel & Mequanint, 2011; Roy & Gupta, 2003). As the polar groups are hydrate, the network swells and exposes the hydrophobic groups that are also capable to interact with water molecules. This leads to the formation of *hydrophobically bound water*, also designated as *secondary bound water*. *Primary* and *secondary bound water* are often combined and denominated *total bound water*. After the water has interacted with both hydrophilic and hydrophobic sites, the osmotic driving force of the network chains allows the network to absorb more water. This additional swelling is opposed by the covalent or physical crosslinks, leading to an elastic network retraction force. At this stage, the hydrogel will reach an equilibrium swelling level. The additional absorbed water beyond the *total bound water* is defined as *free water* or *bulk water* and it is assumed that fills the spaces between the chains and pores (Gulrez, Al-Assaf & O Phillips, 2011; Hoffman, 2002; Patel & Mequanint, 2011; Roy & Gupta,

2003). The water holding capacity of the hydrogels arise mainly due to the presence of hydrophilic groups. As the crosslinking density increases, there is a decrease in the swelling equilibrium due to the diminution of hydrophilic groups available to establish interactions with water. Therefore, the increase in crosslinking density induces an increment in the hydrophobicity and consequently a decrease in the stretchability of the polymer network (Pal, Banthia & Majumdar, 2009).

Hydrogels swell and shrink in presence or absence of an aqueous medium (water or biological fluids), and this process is reversible. Some hydrogels expand or contract in response to specific environmental stimuli, such as, temperature, pH, solvent composition, ionic strength, electric field, light, stress or the presence of specific chemical substances (Jocic, 2008). Thus, these stimuli responsive materials function as on-off switches that are triggered by external impulses/factors (Kopeček, 2002). This molecular switch behaviour opens a wide range of applications for the referred materials. Among the different types of biopolymers, polysaccharides are gaining increasing attention as components of stimuli-responsive hydrogel systems (Alvarez-Lorenzo, Blanco-Fernandez, Puga & Concheiro, 2013). Chitosan (CH) as well as cellulose derivatives, e.g. (hydroxypropyl)methyl cellulose (HPMC), undergo relatively abrupt changes in their swelling behaviour, network structure, permeability and/or mechanical strength in response to small environmental changes, such as pH and temperature, respectively (Patel & Mequanint, 2011). Chitosan is soluble in dilute acids (pH below 5) that protonate the free amino groups. Once dissolved, chitosan can be gelled by increasing the pH to neutral or alkaline conditions (Drury & Mooney, 2003; Francis Suh & Matthew, 2000; Lee & Mooney, 2001). HPMC aqueous solutions (1-10 wt%) are liquid at low temperature but gel upon heating till the low critical solution temperature (LCST) is reached. The HPMC solutions show a phase transition between 75 and 90ºC and the gelation of these solutions is primarily caused by the hydrophobic interaction between molecules containing methoxy substitution (Ruel-Gariépy & Leroux, 2004; Sannino, Demitri & Madaghiele, 2009; Sarkar, 1979).

For textile applications, the most interesting and appealing hydrogel would exhibit smart properties like pH and temperature sensitivity or ideally pH/temperature dual sensitivity. As CH and HPMC are pH and temperature sensitive polymers, respectively, the developed CH:HPMC hydrogels are thus expected to possess both intelligent/interactive properties (Barros et al., 2014). Herein, we characterised these

stimuli responsive hydrogel films in terms of thermal (differential scanning calorimetry (DSC) and thermogravimetric analysis (TGA)) and mechanical analysis (stress-strain mechanical assays and dynamic mechanical analysis (DMA)), as well as, structural studies (X-ray). The designed CH:HPMC membranes, will potentially be applied as an on-off switch, triggered by the human body temperature, to deliver active species, such as antiperspirants, scents and moisturisers, into technical textile applications.

2. Experimental

2.1. Materials

The hydrogels prepared within this study were based in two natural polymers, namely chitosan (CH, 448877) and (hydroxypropyl)methyl cellulose (HPMC, Culminal MHPC 3000), supplied by Sigma-Aldrich Company, Ltd (St. Lois, MO, US) and by Ashland Inc. (Covington, KY, US), respectively. Dilutions of acetic acid (33209, ≥99.8%) purchased to the Sigma-Aldrich Company, Ltd (St. Lois, MO, US) were used both as hydrogel preparation solvent and as pH adjustment solutions. All chemicals were used as purchased, without further purification. Ultrapure water (Milli-Q Gradient A10 Water Purification System, Millipore Corporation, MA, US), with a resistivity >18 $M\Omega.cm^{-1}$ at 25ºC, it was used to prepare all solutions.

2.2. Methods

2.2.1. Hydrogels preparation

The synthesis of the chitosan:(hydroxypropyl)methyl cellulose (CH:HPMC) hydrogels was described in detail elsewhere (Barros et al., 2014). The CH, HPMC and CH:HPMC membranes were prepared by freeze-thaw and solvent casting process. These two methodologies only differ in the last part of the hydrogel preparation procedure. Briefly, CH and HPMC were dissolved in aqueous acetic acid (1 wt%) and ultrapure water, respectively, to prepare 2 wt% CH and HPMC solutions. The CH and HPMC solutions were mixed together in 0:100; 10:90; 20:80; 30:70; 40:60; 50:50; 60:40; 70:30; 80:20; 90:10 and 100:0 (w:w) ratios. These polymeric mixtures were stirred at room

temperature, till a homogeneous solution was achieved. After adjusting the pH of these mixtures to 3.0, 3.5 and 4.0 with a pH meter microprocessor (PH211, Hanna Instruments, Woonsocket, RI, US) and using acetic aqueous solutions with (1:1) and (1:2) proportions, the resulting solutions were casted into 5.5 mm diameter Petri dishes (BP50-01, Gosselin, Hazebrouck, FR). At this phase, the hydrogel films prepared by solvent casting (SC) were exposed to a thermal treatment to promote solvent evaporation, whereas the hydrogel membranes obtained by freeze-thaw were frozen at -20 ºC for 48 hours, followed by defrost till room temperature was reached. The last step in the hydrogel film preparation by both techniques consists in a thermal treatment in an incubator (Infors HT, Minitron, Bottmingen, CH) at: 25 ºC for 5 hours; 40 ºC overnight; 60 ºC during 5 hours and 25 ºC to return the samples to room temperature. This thermal treatment allows a slow solvent evaporation and eliminates the bubbles formed during the pH adjustment procedure. The prepared FT and SC hydrogel films were stored in a desiccator containing silica gel under argon atmosphere. The synthesised hydrogel films (Fig. 1) were designated as CH:HPMC (X:Y), pH Z, FT/SC, where X and Y represents the chitosan and cellulose derivative ratio, Z the pH value being 3.0, 3.5 or 4.0 and FT/SC the membrane preparation technique, freeze-thaw or solvent casting. The membranes thickness ranged between 28-222 ± 1 μm and were measured with a digital micrometer (Mitutoyo 293 series, MDC-25P, Kanagawa, JP).

2.2.2. Thermal analysis

2.2.2.1. Differential scanning calorimetry analysis (DSC)

Differential scanning calorimetry (DSC) measurements were performed in a Mettler Toledo DSC 821^{e} calorimeter (Columbus, OH, US) coupled to a cooling accessory (Labplant cryostat RP-60, Huddersfield, UK). The DSC analyses were conducted over a temperature range of -60 to 400 ºC, at a heating rate of 5 ºC.min^{-1}, under argon purge (50 mL.min^{-1}). Approximately 2 mg of all films were sealed in standard 40 μL aluminium crucibles (Mettler Toledo, ME-26763, Columbus, OH, US). These assays were performed using as reference an empty crucible.

2.2.2.2. Thermogravimetric analysis (TGA)

The thermal stability of the hydrogel films was evaluated by thermogravimetric analysis (TGA) in a Shimadzu TGA-50 (Shimadzu Scientific Instruments, Columbia, MD, US). The thermogravimetric analysis were carried out in a temperature range between 30 and 750ºC, at a heating rate of 10ºC.min^{-1}, under a constant nitrogen flow of 60 mL.min^{-1}. Prior to this assay, samples were subjected to a thermal treatment to eliminate the solvent (water). Thus, the first run was performed from 30 to 105 ºC, at a heating rate of 20 ºC.min^{-1}, followed by a second isothermal run at 105 ºC during 10 min. All analyses were performed using samples with approximately 5 mg in open platinum crucibles/pans.

The differential thermogravimetric (DTG) curve was derived from the TGA results using the Origin 8.5 software program (OriginLab, 2010).

2.2.3. Mechanical and Dynamic mechanical analysis

2.2.3.1. Stress–strain mechanical assays

The mechanical properties of the CH:HPMC membranes were determined using a Linkam TST350 tensile stress testing system (Linkam Scientific Instruments, Surrey, UK) with a load cell of 200 (N), at room temperature. The samples prepared for this assay were film stripes (rectangular shape) with specific dimensions (10x40mm) and free from air bubbles or physical imperfections. These test samples were held between two clamps positioned at a distance of 10mm and during measurement, the sample was pulled by the top clamp at a strain rate of 1 mm.min-^{1}. The tensile strength (σ) was expressed in MPa and calculated by dividing the maximum load (N) by the initial cross-sectional area (m^2) of the film. The elongation at break (ε) was calculated as the ratio of the final length at the point of sample rupture to the initial length of the film (10mm) and expressed as a percentage (Xu, Kim, Hanna & Nag, 2005). The tensile strength and elongation tests were replicated three times for each sample and a mean value was calculated.

2.2.3.2. Dynamic mechanical analysis (DMA)

Dynamic mechanical analyses (DMA) were performed with a Perkin Elmer DMA 8000 instrument (PerkinElmer, Inc; USA). Dynamic mechanical properties were measured from 30 up to 200 ºC, while heating the sample at 2ºC.min^{-1}. Film stripes of about 6 x 4 mm were tested at a frequency of 1 Hz. The dynamic mechanical properties, the mechanical damping tanδ, elastic storage modulus (E') and viscous loss modulus (E''), were evaluated for the CH:HPMC hydrogel films. These assays were performed in triplicated for all film samples analysed.

2.2.4. X-ray diffraction analysis

The X-Ray diffraction measurements were performed at room temperature in a PANalytical X'Pert Pro diffractometer equipped with an X'Celerator detector. The film samples were exposed to monochromated CuKα radiation with λ = 1.541 Å over a scattering angle (2θ) range from 3 to 60º at a scanning rate of º.min^{-1}. In these measurements, samples were placed on a Si wafer, in order to minimise any diffuse scattering from the substrate. The difractograms patterns were fitted using Origin 8.5 program. X-ray diffraction patterns were measured in order to evaluate the crystalline/amorphous character of pure polymers (CH and HPMC) and CH:HPMC hydrogel films.

3. Results and Discussion

3.1. Thermal analysis

3.1.1. Differential scanning calorimetry analysis (DSC)

DSC thermograms of CH and HPMC raw materials and CH:HPMC films are presented in Fig. 2. The DSC curve of unprocessed CH shows a typical polysaccharide behaviour (El-Hefian, Elgannoudi, Mainal & Yahaya, 2010; Guinesi & Cavalheiro, 2006; Kittur, Harish Prashanth, Udaya Sankar & Tharanathan, 2002; Neto, Giacometti, Job, Ferreira, Fonseca & Pereira, 2005; Ruiz-Caro & Veiga-Ochoa, 2009; Synytsya et al., 2009; Tripathi, Mehrotra & Dutta, 2009). The CH thermogram exhibit a broad endothermic peak at T_{onset} of 17.30 ºC that is attributed to water content in the polysaccharide and a sharp exothermic peak at T_{onset} of 277.73 ºC, which is ascribed to the degradation of the chitosan chains. The DSC thermogram of unprocessed HPMC reveals two broad endothermic peaks at T_{onset} of 4.57 ºC and 260.84 ºC, attributed to moisture evaporation from the sample and to polymer decomposition, respectively (Rotta, 2008; Solaiman, 2010). No endothermic melting peaks are observed in the DSC curves of unprocessed CH and HPMC, due to the amorphous state of both polymers (Ruiz-Caro & Veiga-Ochoa, 2009; Solaiman, 2010). All CH:HPMC membranes, prepared by FT and SC method, exhibit a broad endothermic peak centred between 50 and 95 ºC, with a T_{onset} ranging from -20.14 to 24.72 ºC (Table 1). The second thermal event registered in almost all CH:HPMC samples (except for the 10:90 (FT), 0:100, 20:80 and 30:70 (SC) compositions), was also a wide endothermic peak centred between 170 and 205 ºC, with a T_{onset} ranging from 119.02 to 146.45 ºC (Table 1). The first and second endothermic peaks, corresponding to temperature ranges from 50 to 95 ºC and 170 to 205 ºC, respectively, are associated with the loss of the solvent (acetic acid/water) used in the preparation of the samples and the polymers' dehydration process (Qu, Wirsén & Albertsson, 2000; Ruiz-Caro & Veiga-Ochoa, 2009). The above observations support the existence of different states of water in the CH:HPMC films. According to the literature (Cursaru, Stanescu & Teodorescu, 2010; Dhawade & Jagtap, 2012; Joshi & Wilson, 1993; McCrystal, Ford & Rajabi-Siahboomi, 1999; Qu, Wirsén & Albertsson, 2000; Tranoudis & Efron, 2004), water is present in three different forms in a hydrogel. The first one is free water that does not form hydrogen bonds with the polymer and behaves similarly with pure water as far as freezing and melting is concerned. The

second one is freezing bound water, which interacts weakly with the polymer chains and freezes/melts at temperatures shifted with respect to that of free water. The third one is non-freezing bound water that is linked to the polymer chains through hydrogen bonds, and does not exhibit a detectable phase transition within the normal temperature range associated with pure water. The third state of water, so called non-freezing bound water, is postulated to explain the faction of water unaccounted for in DSC measurements (Cursaru, Stanescu & Teodorescu, 2010; McCrystal, Ford & Rajabi-Siahboomi, 1999). To ensure that the first and second endothermic peaks (assigned to free water and freezing bound water, respectively) were correctly attributed to the membrane dehydration, a first and a second DSC scan was registered. The first DSC run was performed in a temperature region below the membranes' thermal degradation (data not shown) (El-Hefian, Elgannoudi, Mainal & Yahaya, 2010; Hussain, Grandy, Reading & Craig, 2004; Neto, Giacometti, Job, Ferreira, Fonseca & Pereira, 2005; Sakurai, Maegawa & Takahashi, 2000). From this study, it was possible to state that the peaks attributed to the dehydration process had disappeared after the first DSC scan. Thus, these two endothermic peaks were accurately associated with the water loss from the CH:HPMC films. In spite of all samples were subjected to the same thermal treatment prior to DSC analysis, the amount of free water (considering the enthalpy (ΔH_{endo}) of the first endothermic peak) varied considerably with the composition and preparation technique (Table 1). Moreover, the lack of information regarding the enthalpy values associated with the second endothermic peak (ascribed to freezing bound water), unable to establish a trend for the water-polymer interaction in the CH:HPMC hydrogel films.

CH and HPMC are hygroscopic polymers (El-Hefian, Elgannoudi, Mainal & Yahaya, 2010; Hussain, Grandy, Reading & Craig, 2004; Kittur, Harish Prashanth, Udaya Sankar & Tharanathan, 2002; Neto, Giacometti, Job, Ferreira, Fonseca & Pereira, 2005), thus inevitably contain a measurable quantity of water. The retained water within the CH:HPMC membranes may act as plasticizer, affecting many properties of the component polymers, such as rheological, transport properties and glass transition temperature (T_g) (Dhawade & Jagtap, 2012; Schubnell & Schawe, 2001). According to literature, the glass transition temperature is dependent upon the amount of moisture in a sample, as moisture not only lowers the temperature at which the transition occurs but also broadens the range over which it is seen (Dhawade & Jagtap, 2012; Ford, 1999; Schubnell & Schawe, 2001; Solaiman, 2010). Thus, the remnant moisture in the

samples might overlap and distorts other thermal events, like the glass transition temperature (T_g) (Dhawade & Jagtap, 2012; Schubnell & Schawe, 2001). In our case, the two broaden endothermic peaks, ascribed to free water and freezing bound water, turned undoable the process to determine the glass transition temperature (T_g) for the developed membranes. Even for the samples in which a second DSC run was performed, the T_g could not be obtained, due to the low sample weight used in this assays (0.5-2.5 mg). Nevertheless, the temperature at which occurs the glass transition for the CH and HPMC biopolymers is not consensual within the research community. According to Dhwade (Dhawade & Jagtap, 2012), the glass transition temperature (T_g) of pure CH appears at 118 ºC, using conventional DSC and at 61 ºC when in presence of water and determined by temperature modulated DSC (MDSC) analysis. These results confirm the fact that water does acts as plasticizer in chitosan (Dhawade & Jagtap, 2012). Ratto *et al* (Ratto, Hatakeyama & Blumstein, 1995) observed the glass transition temperature of CH at 30 °C for water contents ranging from 8 to 30%. Rotta and collaborators (Rotta, Minatti & Barreto, 2011) detected a glass transition temperature for pure CH films at 114.1 ºC, using DSC. Cervera and co-workers (Cervera et al., 2004) found the T_g in CH powder to be around 130 – 139 ºC, by DSC technique. Dong *et al* (Dong, Ruan, Wang, Zhao & Bi, 2004) detected the glass transition temperature for CH films using four different techniques (dynamic mechanical analysis (DMA), differential scanning calorimetry (DSC), thermally stimulated current spectroscopy and dilatometry), reaching a consensual T_g range of 140 to 150 ºC. Chen and collaborates (Chen, Tang, Ning, Wang, Fu & Zhang, 2009) also observed the T_g in CH films around 140 to 150 ºC, using DSC analysis. Sakurai and co-workers (Sakurai, Maegawa & Takahashi, 2000) assigned the glass transition temperature of CH films at 203 ºC using both DSC and DMA techniques. Jiang *et al* (Jiang, Su, Caracci, Bunning, Cooper & Adams, 1996) assumed that the T_g of CH films occurred at $T > 250$ ºC (by DSC), once no glass transition was observed before thermal decomposition. In opposition to all reports, Kittur and collaborators (Kittur, Harish Prashanth, Udaya Sankar & Tharanathan, 2002) detected no glass transition, neither in the first nor in the second DSC heating run (from 20 to 220 ºC) of CH. Thus, considering the wide variety of values of glass transition temperatures attributed to CH films, it was possible to state this event is whether masked by the water loss peaks or by the biomaterial degradation peak.

According to Anuar (Anuar, Wui, Ghodgaonkar & Taib, 2007) unprocessed HPMC evidences a glass transition temperature at 84.9 ºC (using DSC technique), while HPMC films stored under a relative humidity of 25, 50 and 75% present T_g values of 71.4, 69.8 and 54.6 ºC, respectively. The film stored under the highest level of relative humidity had the lowest glass transition temperature, evidencing the plasticizing effect of water in biopolymers like HPMC. Joshi and Wilson (Joshi & Wilson, 1993) evaluated the T_g of dry HPMC films, by DSC, obtaining a value of 154 ºC. In HPMC films containing 1% moisture level, the T_g value decreased to 152 ºC and no glass transition was observed for samples containing greater than 1% of water. Rotta and collaborators (Rotta, Minatti & Barreto, 2011) found the T_g for pure HPMC film at 164.6 ºC, using DSC technique. McPhillips *et al* (McPhillips, Craig, Royall & Hill, 1999) used MDSC to determine the glass transition temperature of HPMC powder obtaining a value of 167.2ºC. In HPMC films, the glass transitions were found to be 165.8 and 165.2 ºC, at a scan rate of 2 and 5 $ºC.min^{-1}$, respectively. Hussain and co-workers (Hussain, Grandy, Reading & Craig, 2004) reported for HPMC films a glass transition temperature at 168 ºC, by MDSC. Solainam (Solaiman, 2010) analysed by MDSC capsule shells of HPMC and detected a T_g ranging from 150 to 159 ºC. Therefore, taking in consideration the temperature range for the HPMC glass transition (between 54.6 and 167.2 ºC) reported herein, it is reasonable to expect that the T_g of HPMC would be masked by the water evaporation peaks. To determine the T_g for the developed CH:HPMC hydrogel films, it was used the dynamic mechanical analysis (DMA, discussed in section 3.2.2) that is a technique that allows the separation of overlapping events, in alternative to conventional DSC.

The DSC thermographs of unprocessed CH and HPMC (shown in Fig. 2) exhibit, at temperatures above 277.73 and 260.84 ºC, an elevation and a decline in the baseline due to CH and HPMC polymer degradation, respectively (Fig. 2). The DSC thermographs of CH films exhibit sharp exothermic decomposition peaks around 300 ºC (Fig. 2), which is in accordance with previous reports (El-Hefian, Elgannoudi, Mainal & Yahaya, 2010; Jiang, Su, Caracci, Bunning, Cooper & Adams, 1996; Sakurai, Maegawa & Takahashi, 2000; Tripathi, Mehrotra & Dutta, 2009). The DSC thermograms of HPMC films show broad endothermic peaks at 296.40 and 299.93 ºC (Fig. 2 and Table 1), attributed to HPMC thermal decomposition that is in agreement with preceding studies (Rotta, 2008; Solaiman, 2010). The CH:HPMC membranes display an endo/exo couplet peak above 297.30 ºC, depending on the polymers proportion in the mixture (Fig. 2 and Table 1).

These data support the fact that the developed hydrogel films have high thermal stability. The membranes decomposition temperatures were further determined by thermogravimetry (TGA), due to the higher sensitivity of the thermogravimetric method to determine this thermal event (TGA detailed discussed is in section 3.1.2).

The DSC thermograms displayed in Fig. 3, for the CH:HPMC (0:100, 50:50, 100:0), pH 3-4, FT/SC membranes, emphasised the fact neither the preparation technique (freeze-thaw or solvent casting) nor the pH variation (pH 3.0; 3.5 or 4.0) induced considerable differences in the thermal behaviour of the CH:HPMC compositions studied.

3.1.2. Thermogravimetric analysis (TGA)

Thermogravimetric analyses (TGA) were carried out in order to evaluate the effect of the physical crosslinking on the thermal stability of CH and HPMC. Fig. 4 a) and b) shows the results of thermogravimetric analysis (TG and DTG curves) for the CH:HPMC hydrogel films prepared by FT and SC techniques, respectively. CH:HPMC membranes exhibit a one-stage degradation process within the temperature range of 270.6 and 348.4 ºC, characterised by a weight loss of about 63.63 to 94.81%. The thermal degradation of pure CH and pure HPMC films usually consists of two stages (Chen, Tang, Ning, Wang, Fu & Zhang, 2009; De Lima, Freire, Fonseca & Pereira, 2009; El-Hefian, Elgannoudi, Mainal & Yahaya, 2010; Neto, Giacometti, Job, Ferreira, Fonseca & Pereira, 2005; Pawlak & Mucha, 2003; Rotta, Minatti & Barreto, 2011; Tripathi, Mehrotra & Dutta, 2009; Yin, Luo, Chen & Khutoryanskiy, 2006). The first thermal event is a weight loss that is related to the evaporation of water present in the sample and the second thermal change is a weight loss associated to the thermal and oxidative decomposition of the base polymers, CH and HPMC. Nevertheless, in our thermograms and derivatograms this first stage is absent due to a thermal treatment that the samples suffer prior to the TGA assay. Samples were subjected to a first TGA run from 30 to 105 ºC, at a heating rate of 20 ºC.min^{-1}, followed by a second isothermal run at 105 ºC, during 10 minutes, as described in section 2.2.2.2. The DTG curves of pure CH films exhibit a thermal event at a temperature maximum of 270.6 and 273.6 ºC, for SC and FT, respectively. These events are associated to the depolymerisation of chitosan chains. Moreover, this CH degradation profile is in good agreement with the results reported by Yin (Yin, Luo, Chen & Khutoryanskiy, 2006) and Rotta (Rotta,

Minatti & Barreto, 2011) that have detected by DTG a maximum degradation rate for CH films at 264 and 307.3 ºC, respectively. The DTG curves of pure HPMC films show a single thermal process at a maximal temperature of 343.5 and 348.4 ºC, for SC and FT, respectively. This process is related to cellulose ethers degradation. The obtained results are in agreement with previous reports that have identified a maximum degradation rate for HPMC films at a temperature of 355 – 356 ºC and 387.9 ºC (Rotta, 2008; Rotta, Minatti & Barreto, 2011; Yin, Luo, Chen & Khutoryanskiy, 2006). The TG and DTG curves evidenced that the CH:HPMC membranes exhibit a degradation behaviour intermediate to those of the pure CH and HPMC films. The decomposition temperature of the CH:HPMC films shifted to higher temperatures with the incorporation of HPMC, indicating that this polymer has a stabilising effect on the degradation of CH. Thus, the physical crosslinking between CH and HPMC polymers increases the thermal stability of the resulting CH:HPCM membranes, comparatively to the CH hydrogel film. This behaviour pointed out that there is a molecular miscibility between these two natural polymers, CH and HPMC. Additionally, these data corroborate with our previous work (Barros et al., 2014), in which the FTIR-ATR and SEM studies have confirmed the miscibility between these two polymers.

According to Fig. 4 a) and b), the CH:HPMC membranes, prepared by FT and SC technique, display a similar thermal decomposition behaviour. Probably, if a higher number of freeze-thaw cycles are implemented, the membranes prepared by this technique would display higher resistance to thermal degradation (Chang & Zhang, 2011; Zhang, Zhang & Wu, 2013). Still, the obtained membranes prepared both by FT and SC techniques, show high thermal stability for the proposed textile application.

Comparing the thermal degradation results obtained by DSC and TG/DTG, we can conclude that they are in very good agreement. Nevertheless, the higher sensitivity of the thermogravimetric method allowed us to determine more accurately the decomposition temperature for the studied membranes, once no baseline variations occur as it commonly happens in the DSC methodology.

3.2. Mechanical/dynamic mechanical properties

3.2.1. Stress–strain mechanical assays

The biodegradability and biocompatibility are the main features of the CH and HPMC based hydrogel films (Bhattarai, Gunn & Zhang, 2010; Sannino, Demitri & Madaghiele, 2009). However, the mechanical properties of such materials are equally important to maintain the structural integrity of the developed membranes (Lazaridou & Biliaderis, 2002). The mechanical properties of hydrogels mainly depend on the original rigidity of polymer chains, types of crosslinking molecules and density, and swelling as a result of hydrophilic/hydrophobic balance (Lee & Mooney, 2001). The mechanical properties tensile strength (σ, strength of the films) and elongation (ε, elasticity of the membranes) of the CH:HPMC membranes were investigated herein, to evaluate the influence that the CH or HPMC incorporation had on the mechanical properties of the resulting materials. The stress-strain curves (tensile strength *versus* elongation graphs) for the CH:HPMC hydrogel films are shown in Fig. 5. In Fig. 6 it is shown the tensile strength and elongation at break for the composite films as a function of CH:HPMC composition. According to Fig. 5 and 6, the pure CH films, prepared both by FT and SC, exhibit the lowest tensile strength (3.68 and 4.63 MPa, respectively), revealing the low mechanical resistance of these membranes. Whereas, the pure HPMC films attained by FT and SC displayed the highest tensile strength values (6.85 and 8.15 MPa, respectively). These results suggest that pure HPMC films are almost twice resistant than the pure CH films. According to literature, physically crosslinked hydrogels that present high swelling ratios, display low mechanical strength, due to the weak hydrogen bonding between the component polymers (Anseth, Bowman & Brannon-Peppas, 1996; Bhattarai, Gunn & Zhang, 2010; Chang & Zhang, 2011; Pal, Banthia & Majumdar, 2009). These data corroborate with our previous studies (Barros et al., 2014) in which we have found that the CH:HPMC hydrogels with higher CH content, displayed higher swelling capacity. Therefore, as confirmed herein, lower mechanical properties were expected for these compositions. In the CH:HPMC hydrogel films, prepared by FT technique, the maximum enhancement in tensile strength of 7.07 MPa was reached for the 50:50 composition, as a result of the good/excellent intermolecular interaction between these two polymers. The mechanical strength of these physical hydrogels might be improved by repeating freezing/thawing cycles that increase the crosslinking density between the constituent polymers (Chang & Zhang, 2011). For the CH:HPMC

membranes, attained by SC process, the tensile strength profile is different from the obtained by FT methodology. These composite films exhibit a maximum and a minimum value of tensile strength for pure HPMC and pure CH films, respectively. These results might suggest the inexistence of polymer-polymer interactions, which it is not in accordance with our previous studies of swelling, FTIR-ATR and SEM (Barros et al., 2014).

Regarding the elongation at break (ε), the CH:HPMC membranes obtained by FT and SC exhibited a minimum value for the composition 50:50 (5.93 and 5.60%, respectively) and maximum elongation values for the 100:0 (13.13 and 18.53%, respectively) and 0:100 (11.67 and 11.07%, respectively) compositions. The low elasticity shown for the CH:HPMC(50:50) composition, might be attributed to the presence of intermolecular interactions between the two component polymers, *i.e.*, hydrogen bonds between the -NH_2 and -OH groups of CH and HPMC polymers, respectively (Chen, Tang, Ning, Wang, Fu & Zhang, 2009; Pal, Banthia & Majumdar, 2009; Parida, Nayak, Binhani & Nayak, 2011). Considering the high content of both polymers in the CH:HPMC(50:50) composition, it was thus expected a high crosslinking density for this composition. These results are in accordance with our previous swelling studies (Barros et al., 2014), in which we have disclosed that the lowest swelling capacities were attained for the CH:HPMC compositions with equivalent contents of both polymers. Rotta and co-workers (Rotta, Minatti & Barreto, 2011) have reported for the CH:HPMC hydrogel films higher values of tensile strength and lower values of elongation at break ($\sigma_{(100:0)}$= 35 MPa and $\sigma_{(0:100)}$= 21 MPa; $\varepsilon_{(100:0)}$= 1.9 % and $\varepsilon_{(0:100)}$= 5.1 %, using a load cell of 200 kgf), under similar experimental conditions.

For the CH:HPMC(50:50), FT and SC prepared at different pH values (3.0, 3.5 and 4.0), it is noticed a similar tensile strength and elongation at break pattern (Fig. 5 and 6). The highest strength and elasticity is attained for the CH:HPMC (50:50) hydrogel films prepared at pH 3.5 ($\sigma_{(50:50,\ FT)}$= 8.42 MPa and $\sigma_{(50:50,\ SC)}$= 7.70 MPa; $\varepsilon_{(50:50,\ FT)}$= 20.48 % and $\varepsilon_{(50:50,\ SC)}$= 18.27 %).

3.2.2. Dynamic mechanical analysis (DMA)

The dynamic mechanical analysis (DMA) yields values of elastic or storage modulus (E'), viscous or loss modulus (E'') and mechanical loss tangent or dissipation factor (Tan δ = E''/E'). The E' values provide information about the energy stored in the material during deformation stress, while E" describes its viscous character (Pasqui, De Cagna & Barbucci, 2012). The trends of storage modulus (E'), and dissipation factor (Tan δ) as a function of the temperature, for the CH:HPMC hydrogel films are illustrated in Fig. 7 and 8.

The storage modulus E' is higher in SC samples than in FT ones, the former showing at room temperatures values in the order of those expected for a glassy polymer. Nevertheless the absolute values of the elastic modulus of hydrogels are highly dependent on the water content and the differences found could not be related to changes in the molecular structure.

All the samples show an increase of the elastic modulus with temperature in the range between room temperature and 100ºC. This phenomenon must be ascribed to the loss of water on heating already detected in DSC thermograms. As water leaves the sample its stiffness increases as expected.

No relaxation processes appear in the pure CH sample while in and HPMC FT sample there appear a drop in the elastic modulus around 160ªC but it is not accompanied of a clear peak in the loss tangent due to the beginning of sample degradation so the interpretation is not clear. Sample degradation is responsible for the distortion of the measurements at the highest temperatures of the scan.

Interestingly, the decrease of pH in the preparation of samples produces a clear relaxation process in both SC and FT samples in 50/50 blend, detected as a peak in tanδ and a large drop in logE' (Figure 8). This process can be ascribed to the main dynamic mechanical relaxation process which is due to conformational rearrangements of the amorphous part of the polymer segments. The maximum in the tanδ against temperature plot Tα measured at 1 Hz could appear around 30ºC above the glass transition temperature T_g measured by DSC. The peak shown in the loss tangent in the range of temperatures between 0 and 100ºC could be an artefact produced by the increase in E' due water evaporation and not a relaxation process.

The E’ and E’’ *versus* temperature curves for the developed membranes (Fig. 7 a-d)) show a solid-like behaviour, *i.e.*, the elastic properties dominate over the viscous properties and consequently the storage modulus (E’) values are higher than the loss modulus (E’’). Moreover, the obtained E’ and E’’ values are considerably high and the presented curves are practically parallel. According to Pal and collaborators (Pal, Banthia & Majumdar, 2009), hydrogels that are highly crosslinked polymer networks, both E’ and E” are very high and are nearly parallel to each other. Thus, these results evidence the fact that the CH:HPMC hydrogels films attained by FT and SC techniques, display a high physical crosslink density. Furthermore, neither the different preparation technique FT and SC (Fig. 7), nor the pH variation between 3.0 and 4.0 (Fig. 8), induced considerable changes in the storage and loss modulus profile.

Fig. 7 e-f) show the temperature dependence of the Tan δ values of CH:HPMC membranes, prepared both by FT and SC methodologies. It is generally accepted that the temperature at the maximum value in Tan δ corresponds to the glass–rubber transition (Wu 2004). Therefore, the Tan δ peaks at 194.5 and 193.9 ºC in the CH:HPMC (0:100), pH 4.0, FT and SC curves, are related to the molecular motion in the amorphous region and are ascribed to the glass transition temperature (T_g) of HPMC. According to Wu and co-workers (Wu et al., 2004) the Tan δ peak for cellulose films occurred at 190 ºC, which corroborates with results reported herein.

The CH:HPMC (100:0), pH 4.0, FT and SC curves, evidence no Tan δ peaks within the studied temperature range (between 30 and 200 ºC), evidencing the absence of a glass transition attributed to CH. According to Jiang *et al* (Jiang, Su, Caracci, Bunning, Cooper & Adams, 1996), the DSC thermogram of CH does not show a glass transition before thermal decomposition (T > 250 ºC), due to its semi-rigid molecular backbone. Sakurai and collaborators (Sakurai, Maegawa & Takahashi, 2000) identified by DSC and DMA (in a second heating run) a glass transition temperature for CH at 203 and 205 ºC, respectively. Moreover, Barreiro-Iglesias and coworkers (Barreiro-Iglesias, Coronilla, Concheiro & Alvarez-Lorenzo, 2005) also identified by DMA measurements (in a second heating run) a relaxation temperature for CH at 205 ºC. Considering the structural similarity between chitin and its derivative polymer chitosan, it is thus expected a similar glass transition temperature for these materials. Kim et al (Kim, Kim, Moon & Lee, 1994) estimated the T_g of chitin to be 236 ºC from the Tan δ curve based on DMA. Therefore all these studies pointed out that the CH glass transition

temperature might be above 200 ºC and justify the absence of a T_g peak in the Tan δ curves of CH.

Considering this approach, it is thus expected that the CH:HPMC (30:70, 50:50 and 70:30) compositions exhibit no Tan δ peaks ascribed to glass transition temperature. The results shown in Fig 7 e-f corroborate this statement. These CH:HMPC mixtures might exhibit a glass transition temperature intermediate to the component polymers, considering a good miscibility between CH and HPMC. If these mixtures are immiscible, they should display two glass transition peaks correspondent to each component polymer. In our case, the studied CH:HPMC membranes revealed a good compatibility between the component polymers (Barros et al., 2014) and therefore a single T_g is expected, between 194 and ~ 250 ºC, for the CH:HPMC mixtures.

3.3. X-ray diffraction analysis

X-ray diffraction or X-ray diffractometry (XRD) is a technique that can be used to distinguish between ordered and disordered materials and therefore, yields very useful information on the degree of sample crystallinity (Robinson, Frame & Frame II, 2005; Tripathi, Mehrotra & Dutta, 2009). X-ray diffraction patterns of CH and HPMC powder and CH:HPMC hydrogel films (FT and SC) are shown in Fig. 8. The diffractogram of powdered chitosan has two diffraction peaks at 2θ = 9.86º and 20.06º, thus confirming the presence of crystalline domains in its structure. These values are very similar to those found by Xu and collaborators (Xu, Kim, Hanna & Nag, 2005), at 2θ = 11.6º and 20.25º. The X-ray diffraction pattern of the CH films (FT and SC) exhibit the same two crystalline peaks at $2\theta_{(FT)}$ = 9.08º and 19.06º and $2\theta_{(SC)}$ = 11.74º and 20.10º, however with much lower intensities. Chitosan is a partially crystalline polymer (Cervera et al., 2004; Sakurai, Maegawa & Takahashi, 2000), thus there might exist a small amount of crystallites in the CH films. The crystallites in the CH films could be from two different sources. The first one are the original anhydrous crystals in the raw material, which are difficult to dissolve in acidic solutions and may remain in the final films. The second one is that some degree of aggregation of the rigid chitosan molecules could occur in the dilute acetic acid solution. During processing, with the evaporation of solvents, the aggregation might act as the nuclei to form small crystallites (Jiang, Su, Caracci, Bunning, Cooper & Adams, 1996).

The diffraction profile of powdered HPMC exhibit two broad diffraction peaks at 8.52º and 20.26º, evidencing the low crystallinity of this material. These results agree with the findings reported by Hino and Ford (Hino & Ford, 2001), which have shown that HPMC is mostly amorphous. Their findings are based on the presence of two widen peaks at approximately 10º and 20º in the X-ray diffractogram of solid HPMC. The X-ray diffraction pattern of the HPMC films (FT and SC) also exhibit these two broaden diffraction peaks, however as these peaks had very low intensities, it was undoable to determine the 2θ value for the first diffraction peak ($2\theta_{(FT)} \approx 10º$ and 20.56º and $2\theta_{(SC)} \approx 10º$ and 20.12º). These results evidence the amorphous nature of the HPMC films and are in good agreement with those reported by Rotta *et al* (Rotta, Minatti & Barreto, 2011) (2θ = 11.7º and 20.18º), Yin *et al* (Yin, Luo, Chen & Khutoryanskiy, 2006) and Loh *et al* (Loh, Tan & Peh, 2014) that have identified two widen diffraction peaks at approximately 10º and 20º for pure HPMC films.

The CH:HPMC hydrogel films (FT and SC) reveal a X-ray diffraction pattern intermediate to those of the pure polymer (CH and HPMC) films. This can be considered as an indicative on the miscibility between these two polymers. According to Yin (Yin, Luo, Chen & Khutoryanskiy, 2006) and Rotta (Rotta, Minatti & Barreto, 2011), the shift of diffraction angles and a change in the peaks intensity, can be considered an evidence of a partial miscibility between polymers. The diffractograms of CH:HPMC membranes exhibit two large diffraction peaks of $2\theta_{(FT\&SC)}$ = 9.04-12.84º and 20.12-21.24º with very low intensities, revealing the amorphous nature of these membranes. These findings are consistent with the DSC results that have shown the amorphous state of these CH:HPMC films, due to the absence of endothermic melting peaks. The diffractograms of all CH:HPMC membranes (except for the CH:HPMC (30:70), FT composition) display a sharp and intense peak at 2θ = 32.94º that corresponds to the silicon substrate used in X-ray measurements (Slama, Hajji & Ezzaouia, 2012).

4. Conclusions

The hydrogel films composed of chitosan (CH) and (hydroxypropyl)methyl cellulose (HPMC) with different compositions have been successfully prepared via freeze-thaw (FT) and solution-casting (SC) techniques. The developed CH:HPMC films were evaluated in terms of thermal (DSC and TGA) mechanical (stress-strain mechanical assays and DMA) and structural properties (X-ray). The obtained results evidenced that the developed thermoreversible membranes display an excellent thermal stability, good mechanical properties and an amorphous character.

The DSC analysis of the CH:HPMC films revealed the existence of two broad endothermic peaks in the 50 – 95 ºC and 170 – 205 ºC intervals (peak temperature), attributed to moisture (water) evaporation. An endo/exo couplet peak at T > 297.30 ºC, ascribed to polymer (HPMC and CH) decomposition, was also observed. The thermostability and degradation of the membranes were assessed by TGA that corroborate with the DSC studies. The TG and DTG curves for these membranes, exhibited a one-stage degradation process within the temperature range of 270.6 - 348.4 ºC and this weight loss was associated with the decomposition of the base polymers, CH and HPMC. Moreover, the TG and DTG curves evidenced that the CH:HPMC films exhibited a degradation behaviour intermediate to those of the pure components films. This behaviour pointed out that there is a molecular miscibility between the two component polymers, CH and HPMC. The X-ray studies also supports this statement, based on the fact that the CH:HPMC membranes showed a X-ray diffraction pattern intermediate to those of the pure polymer (CH and HPMC) films. The diffractograms of CH:HPMC films exhibited two broad diffraction peaks of $2\theta_{(FT\&SC)}$ = 9.04-12.84º and 20.12-21.24º with very low intensities, revealing the amorphous nature of these membranes.

The dynamic mechanic analysis (DMA), was employed within this work to allow the determination of the glass transition temperature (T_g) for the CH:HPMC membranes that was undoable by DSC. In DSC analysis, this thermal event was weather masked by the solvent (water) evaporation or by polymer decomposition peak. The DMA analysis revealed that HPMC films displayed a T_g at 194.5 and 193.9 ºC, whereas the CH films exhibit no T_g within the studied temperature range (30 – 200 ºC). The CH:HPMC membranes, as the CH films revealed no T_g, however a single T_g is expected to occur in

between the CH and HPMC T_g values (194 - ~ 250 º). This fact can be considered as another indicative on the miscibility between these two polymers, otherwise two T_g values, correspondent to CH and HPMC, respectively, would be expected to appear. These results, along with those obtained by TGA and X-ray, and the previously reported FTIR-ATR and SEM studies (Barros et al., 2014), emphasise the good compatibility between the two constituent biopolymers.

Regarding the mechanical properties, tensile strength (σ, strength of the films) and elongation (ε, elasticity of the membranes), of the CH:HPMC films, the composition 50:50 reached the maximum in tensile strength with σ = 7.07 MPa and the minimum in elongation with ε = 5.93 - 5.60%. Considering the high content of both polymers in the CH:HPMC(50:50) composition, it was thus expected a high crosslinking density for this composition and consequently a good tensile resistance. The low elasticity shown for the CH:HPMC(50:50) composition, might be attributed to the presence of intermolecular interactions between the two component polymers, *via* hydrogen bonds between the $-NH_2$ and -OH groups of CH and HPMC, respectively.

In summary, the CH:HPMC membranes exhibit good thermal and mechanical properties and a predominant amorphous character. These properties make the developed thermoreversible films appropriated candidates for the proposed textile application, as delivers of active species, such as scents, moisturisers and antiperspirants.

Acknowledgements

The authors are thankful to the Chemistry and Physic Centres at Minho University (Pest-C/QUI/UI0686/2013 and PEST-C/FIS/UI607/2013), CNPq, FAPESP and CAPES for the financial support of this research. Sandra Cerqueira Barros and Carlos M. Costa acknowledge the Portuguese Foundation for Science and Technology for the Post-Doc and PhD grants provided (SFRH/BPD/85399/2012 and SFRH/BD/68499/2010) and M. M. Silva acknowledges to CNPq, for the mobility grant provided by this institution. The authors of this paper are grateful to the Company Devan-Micropolis, S.A., for the material support, namely the natural polymers chitosan (CH) and (hydroxypropyl)methyl cellulose (HPMC) employed in this study. JLGR acknowledges

the support of Ministerio de Economía y Competitividad, MINECO, through the MAT2013-46467-C4-1-R project. CIBER-BBN is an initiative funded by the VI National R&D&i Plan 2008-2011, Iniciativa Ingenio 2010, Consolider Program, CIBER Actions and financed by the Instituto de Salud Carlos III with assistance from the European Regional Development Fund.

References

Alvarez-Lorenzo, C., Blanco-Fernandez, B., Puga, A. M., & Concheiro, A. (2013). Crosslinked ionic polysaccharides for stimuli-sensitive drug delivery. *Advanced Drug Delivery Reviews, 65*(9), 1148-1171.

Anseth, K. S., Bowman, C. N., & Brannon-Peppas, L. (1996). Mechanical properties of hydrogels and their experimental determination. *Biomaterials, 17*(17), 1647-1657.

Anuar, N. K., Wui, W. T., Ghodgaonkar, D. K., & Taib, M. N. (2007). Characterization of hydroxypropylmethylcellulose films using microwave non-destructive testing technique. *Journal of Pharmaceutical and Biomedical Analysis, 43*(2), 549-557.

Barreiro-Iglesias, R., Coronilla, R., Concheiro, A., & Alvarez-Lorenzo, C. (2005). Preparation of chitosan beads by simultaneous cross-linking/insolubilisation in basic pH: rheological optimisation and drug loading/release behaviour. *European Journal of Pharmaceutical Sciences, 24*(1), 77-84.

Barros, S. C., Silva, A. A., Costa, D. B., Cesarino, I., Costa, C. M., Mendez, S. L., Pawlicka, A., & Silva, M. M. (2014). Thermo-sensitive chitosan-cellulose hydrogels: swelling behaviour and morphologic studies. *Submitted to Cellulose*.

Bhattarai, N., Gunn, J., & Zhang, M. (2010). Chitosan-based hydrogels for controlled, localized drug delivery. *Advanced Drug Delivery Reviews, 62*(1), 83-99.

Cervera, M. F., Heinämäki, J., Räsänen, M., Maunu, S. L., Karjalainen, M., Acosta, O. M. N., Colarte, A. I., & Yliruusi, J. (2004). Solid-state characterization of chitosans derived from lobster chitin. *Carbohydrate Polymers, 58*(4), 401-408.

Chang, C., & Zhang, L. (2011). Cellulose-based hydrogels: present status and application prospects. *Carbohydrate Polymers, 84*(1), 40-53.

Chen, L., Tang, C.-y., Ning, N.-y., Wang, C.-y., Fu, Q., & Zhang, Q. (2009). Preparation and properties of chitosan/lignin composite films *Chinese Journal of Polymer Science, 27*(05), 739-746.

Cursaru, B., Stanescu, P. O., & Teodorescu, M. (2010). The states of water in hydrogels synthesized from diepoxy-terminated poly/ethylene glycol)s and aliphatic polyamines. *UPB Scientific Bulletin, Series B, 72*(4), 99-114.

De Lima, M. S. P., Freire, M. S., Fonseca, J. L. C., & Pereira, M. R. (2009). Chitosan membranes modified by contact with poly(acrylic acid). *Carbohydrate Research, 344*(13), 1709-1715.

Dhawade, P. P., & Jagtap, R. N. (2012). Characterization of the glass transition temperature of chitosan and its oligomers by temperature modulated differential scanning calorimetry. *Advances in Applied Science Research, 3*(3), 1372-1382.

Dong, Y., Ruan, Y., Wang, H., Zhao, Y., & Bi, D. (2004). Studies on glass transition temperature of chitosan with four techniques. *Journal of Applied Polymer Science, 93*(4), 1553-1558.

Drury, J. L., & Mooney, D. J. (2003). Hydrogels for tissue engineering: scaffold design variables and applications. *Biomaterials, 24*(24), 4337-4351.

El-Hefian, E. A., Elgannoudi, E. S., Mainal, A., & Yahaya, A. H. (2010). Characterization of chitosan in acetic acid: rheological and thermal studies. *Turkish Journal of Chemistry, 34*(1), 47-56.

Ford, J. L. (1999). Thermal analysis of hydroxypropylmethylcellulose and methylcellulose: powders, gels and matrix tablets. *International Journal of Pharmaceutics, 179*(2), 209-228.

Francis Suh, J. K., & Matthew, H. W. T. (2000). Application of chitosan-based polysaccharide biomaterials in cartilage tissue engineering: a review. *Biomaterials, 21*(24), 2589-2598.

Guinesi, L. S., & Cavalheiro, É. T. G. (2006). The use of DSC curves to determine the acetylation degree of chitin/chitosan samples. *Thermochimica Acta, 444*(2), 128-133.

Gulrez, S. K. H., Al-Assaf, S., & O Phillips, G. (2011). *Hydrogels: methods of preparation, characterisation and applications,* . InTech.

Hino, T., & Ford, J. L. (2001). Characterization of the hydroxypropylmethylcellulose–nicotinamide binary system. *International Journal of Pharmaceutics, 219*(1–2), 39-49.

Hoare, T. R., & Kohane, D. S. (2008). Hydrogels in drug delivery: Progress and challenges. *Polymer, 49*(8), 1993-2007.

Hoffman, A. S. (2002). Hydrogels for biomedical applications. *Advanced Drug Delivery Reviews, 54*(1), 3-12.

Hussain, S., Grandy, D. B., Reading, M., & Craig, D. Q. M. (2004). A study of phase separation in peptide-loaded HPMC films using Tzero-modulated temperature DSC, atomic force microscopy, and scanning electron microscopy. *Journal of Pharmaceutical Sciences, 93*(7), 1672-1681.

Jiang, H., Su, W., Caracci, S., Bunning, T. J., Cooper, T., & Adams, W. W. (1996). Optical waveguiding and morphology of chitosan thin films. *Journal of Applied Polymer Science, 61*(7), 1163-1171.

Jocic, D. (2008). Smart textile materials by surface modification with biopolymeric systems. *Research Journal of Textile and Apparel, 12*(2), 58-65.

Joshi, H. N., & Wilson, T. D. (1993). Calorimetric studies of dissolution of hydroxypropyl methylcellulose E5 (HPMC E5) in water. *Journal of Pharmaceutical Sciences, 82*(10), 1033-1038.

Kim, S. S., Kim, S. J., Moon, Y. D., & Lee, Y. M. (1994). Thermal characteristics of chitin and hydroxypropyl chitin. *Polymer, 35*(15), 3212-3216.

Kittur, F. S., Harish Prashanth, K. V., Udaya Sankar, K., & Tharanathan, R. N. (2002). Characterization of chitin, chitosan and their carboxymethyl derivatives by differential scanning calorimetry. *Carbohydrate Polymers, 49*(2), 185-193.

Kopeček, J. (2002). Polymer chemistry: swell gels. *Nature, 417*(6887), 388.

Lazaridou, A., & Biliaderis, C. G. (2002). Thermophysical properties of chitosan, chitosan–starch and chitosan–pullulan films near the glass transition. *Carbohydrate Polymers, 48*(2), 179-190.

Lee, K. Y., & Mooney, D. J. (2001). Hydrogels for tissue engineering. *Chemical Reviews, 101*(7), 1869-1880.

Loh, G. O. K., Tan, Y. T. F., & Peh, K. K. (2014). Effect of HPMC concentration on β-cyclodextrin solubilization of norfloxacin. *Carbohydrate Polymers, 101*(0), 505-510.

McCrystal, C. B., Ford, J. L., & Rajabi-Siahboomi, A. R. (1999). Water distribution studies within cellulose ethers using differential scanning calorimetry. 2. Effect of polymer substitution type and drug addition. *Journal of Pharmaceutical Sciences, 88*(8), 797-801.

McPhillips, H., Craig, D. Q. M., Royall, P. G., & Hill, V. L. (1999). Characterisation of the glass transition of HPMC using modulated temperature differential scanning calorimetry. *International Journal of Pharmaceutics, 180*(1), 83-90.

Neto, C. G. T., Giacometti, J. A., Job, A. E., Ferreira, F. C., Fonseca, J. L. C., & Pereira, M. R. (2005). Thermal analysis of chitosan based networks. *Carbohydrate Polymers, 62*(2), 97-103.

OriginLab, C. (2010). OriginPro. Northampton.

Pal, K., Banthia, A. K., & Majumdar, D. (2009). Polymeric hydrogels: characterization and biomedical applications - a mini review. *Designed Monomers and Polymers, 12*, 197-220.

Parida, U. K., Nayak, A. K., Binhani, B. K., & Nayak, P. L. (2011). Synthesis and characterization of chitosan-polyvinyl alcohol blended with cloisite 30B for controlled release of the anticancer drug curcumin. *Journal of Biomaterials and Nanobiotechnology, 2*(4), 414-425.

Pasqui, D., De Cagna, M., & Barbucci, R. (2012). Polysaccharide-based hydrogels: the key role of water in affecting mechanical properties. *Polymers, 4*(3), 1517-1534.

Patel, A., & Mequanint, K. (2011). *Hydrogel biomaterials*. InTech.

Pawlak, A., & Mucha, M. (2003). Thermogravimetric and FTIR studies of chitosan blends. *Thermochimica Acta, 396*(1–2), 153-166.

Qu, X., Wirsén, A., & Albertsson, A. C. (2000). Novel pH-sensitive chitosan hydrogels: swelling behavior and states of water. *Polymer, 41*(12), 4589-4598.

Ratto, J., Hatakeyama, T., & Blumstein, R. B. (1995). Differential scanning calorimetry investigation of phase transitions in water/ chitosan systems. *Polymer, 36*(15), 2915-2919.

Robinson, J. W., Frame, E. M. S., & Frame II, G. M. (2005). Undergraduate instrumental analysis. In M. Dekker (Ed.). New York: Taylon & Francis e-Library.

Rotta, J. (2008). Propriedades físico-químicas de soluções formadoras e de filmes de quitosana e hidroxipropilmetilcelulose (Vol. Master Thesis). Florianópolis: Universidade Federal de Santa Catarina.

Rotta, J., Minatti, E., & Barreto, P. L. M. (2011). Determination of structural and mechanical properties, diffractometry, and thermal analysis of chitosan and hydroxypropylmethylcellulose (HPMC) films plasticized with sorbitol. *SBCTA, 31*(2).

Roy, I., & Gupta, M. N. (2003). Smart Polymeric Materials: Emerging Biochemical Applications. *Chemistry & Biology, 10*(12), 1161-1171.

Ruel-Gariépy, E., & Leroux, J.-C. (2004). In situ-forming hydrogels—review of temperature-sensitive systems. *European Journal of Pharmaceutics and Biopharmaceutics, 58*(2), 409-426.

Ruiz-Caro, R., & Veiga-Ochoa, M. D. (2009). Characterization and dissolution study of chitosan freeze-dried systems for drug controlled release. *Molecules, 14*(11), 4370-4386.

Sakurai, K., Maegawa, T., & Takahashi, T. (2000). Glass transition temperature of chitosan and miscibility of chitosan/poly(N-vinyl pyrrolidone) blends. *Polymer, 41*(19), 7051-7056.

Sannino, A., Demitri, C., & Madaghiele, M. (2009). Biodegradable cellulose-based hydrogels: design and applications. *Materials, 2*(2), 353-373.

Sarkar, N. (1979). Thermal gelation properties of methyl and hydroxypropyl methylcellulose. *Journal of Applied Polymer Science, 24*(4), 1073-1087.

Schubnell, M., & Schawe, J. E. K. (2001). Quantitative determination of the specific heat and the glass transition of moist samples by temperature modulated differential scanning calorimetry. *International Journal of Pharmaceutics, 217*(1–2), 173-181.

Slama, S. B., Hajji, M., & Ezzaouia, H. (2012). Crystallization of amorphous silicon thin films deposited by PECVD on nickel-metalized porous silicon. *Nanoscale Research Letters, 7*(1), 1-6.

Solaiman, A. (2010). Properties of Capsule Shells made from Hydroxypropyl Methylcellulose (Hypromellose). (Vol. Doctor of Philosophy): University of Sunderland.

Synytsya, A., Synytsya, A., Blafková, P., Ederová, J., Spěvaček, J. i., Slepička, P., Král, V. r., & Volka, K. (2009). pH-controlled self-assembling of meso-tetrakis(4-

sulfonatophenyl)porphyrin−chitosan complexes. *Biomacromolecules, 10*(5), 1067-1076.

Tranoudis, I., & Efron, N. (2004). Water properties of soft contact lens materials. *Contact Lens and Anterior Eye, 27*(4), 193-208.

Tripathi, S., Mehrotra, G. K., & Dutta, P. K. (2009). Physicochemical and bioactivity of cross-linked chitosan–PVA film for food packaging applications. *International Journal of Biological Macromolecules, 45*(4), 372-376.

Wu, Y.-B., Yu, S.-H., Mi, F.-L., Wu, C.-W., Shyu, S.-S., Peng, C.-K., & Chao, A.-C. (2004). Preparation and characterization on mechanical and antibacterial properties of chitsoan/cellulose blends. *Carbohydrate Polymers, 57*(4), 435-440.

Xu, Y. X., Kim, K. M., Hanna, M. A., & Nag, D. (2005). Chitosan–starch composite film: preparation and characterization. *Industrial Crops and Products, 21*(2), 185-192.

Yin, J., Luo, K., Chen, X., & Khutoryanskiy, V. V. (2006). Miscibility studies of the blends of chitosan with some cellulose ethers. *Carbohydrate Polymers, 63*(2), 238-244.

Zhang, H., Zhang, F., & Wu, J. (2013). Physically crosslinked hydrogels from polysaccharides prepared by freeze–thaw technique. *Reactive and Functional Polymers, 73*(7), 923-928.

Figure and table list

Fig. 1. Image of the CH:HPMC (X:Y), pH 4.0 hydrogel films obtained by SC, for the polymeric compositions 100:0, 50:50 and 0:100.

Or

Image of the CH:HPMC (100:0, 50:50 and 0:100), pH 4.0 hydrogel films obtained by SC methodology.

Fig. 2. DSC curves of the CH:HPMC (X:Y), pH 4 hydrogel films, prepared by a) FT and b) SC technique. These assays were performed in a Mettler Toledo DSC 821^{e} dynamic scanning calorimeter, at a temperature range of -60 to 400ºC and heating rate of 5ºC.min^{-1}, under argon atmosphere (50 ml.min^{-1}).

Fig. 3. DSC thermograms of the CH:HPMC (X:Y), pH 3-4 hydrogel films, obtained by a) FT and b) SC, for the polymeric compositions 0:100, 50:50 and 100:0.

Or

Fig. 3. DSC thermograms of the CH:HPMC (0:100, 50:50 and 100:0), pH 3-4 hydrogel films, obtained by a) FT and b) SC techniques.

Fig. 4. TGA and DTG thermograms of the CH:HPMC (X:Y), pH4 hydrogel films, for the compositions 100:0, 10:90, 30:70, 50:50, 70:30, 90:10 and 100:0, attained by a) FT and b) SC. These assays were performed in a Shimadzu TGA-50 equipment, at a temperature range between 30 and 750ºC and a heating rate of 10ºC.min^{-1}, under nitrogen purge (50 mL/min).

Fig. 5. Stress-strain curves (tensile strength (σ) *versus* elongation (ε)) and composition influence on tensile strength and elongation at break for the CH:HPMC hydrogel films, prepared by a) FT and b) SC techniques. These assays were performed in a Linkam

TST350 tensile stress testing system with a load cell of …Newtons (N), at room temperature. At least three measurements of tensile strength and elongation at break were recorded for each membrane analysed and a mean value was calculated.

Fig. 6. Stress-strain curves and composition influence on tensile strength (σ) and elongation (ε) at break of the CH:HPMC (50:50), FT and SC membranes, prepared at different pH values (3.0, 3.5 and 4.0).

Fig. 7. Rheological behaviour of CH:HPMC (X:Y), pH 4 hydrogel films, prepared by a, c, e) FT and b, d, f) SC techniques. These assays were performed in a Seiko DMS210 instrument, from 30 up to 200 ºC, at a heating rate of 2 ºC.min^{-1} and a frequency of 1 Hz, in tensile mode.

Fig. 8. Dynamic mechanical spectra of CH:HPMC (50:50), pH 3-4 hydrogel films, attained by FT and SC process.

Fig. 9. X-ray diffraction patterns of CH:HPMC (X:Y), pH 4.0 a) FT and b) SC hydrogel films and CH and HPMC polymers. These assays were performed in a PANalytical X'Pert Pro instrument with Cu Kα (λ=1,541 Å) radiation, over a range of diffraction angle (2θ) from 3 to 60º.

Table 1: DSC thermal events of CH:HPMC (X:Y), pH 4, FT and SC hydrogel films.

Figures CH:HPMC (X:Y), pH Z system

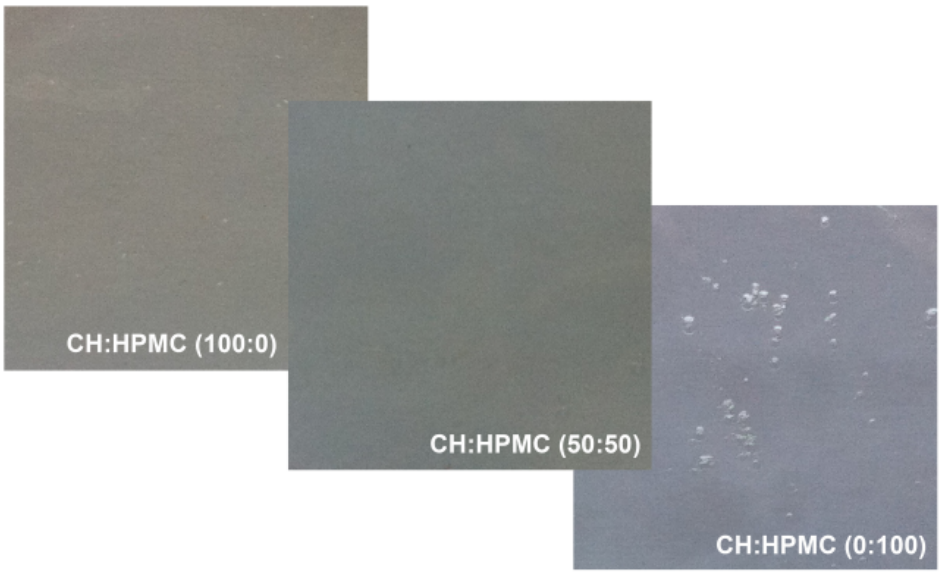

Figure 1. Image of the CH:HPMC (X:Y), pH 4.0 hydrogel films obtained by SC, for the polymeric compositions 100:0, 50:50 and 0:100.

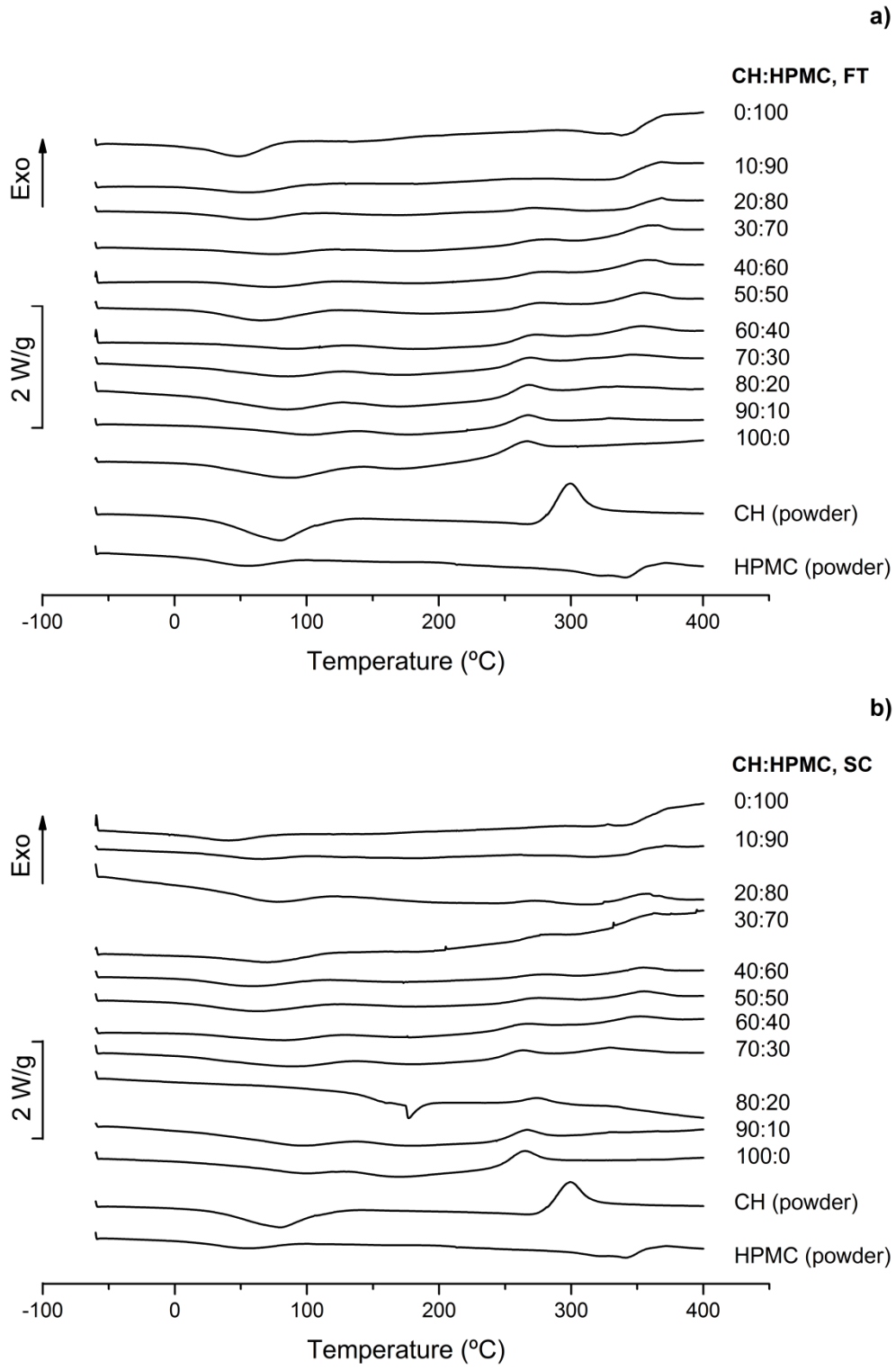

Figure 2. DSC curves of the CH:HPMC (X:Y), pH 4 hydrogel films, prepared by a) FT and b) SC technique. These assays were performed in a Mettler Toledo DSC 821^{e} dynamic scanning calorimeter, at a temperature range of -60 to 400ºC and heating rate of 5ºC.min^{-1}, under argon atmosphere (50 ml.min^{-1}).

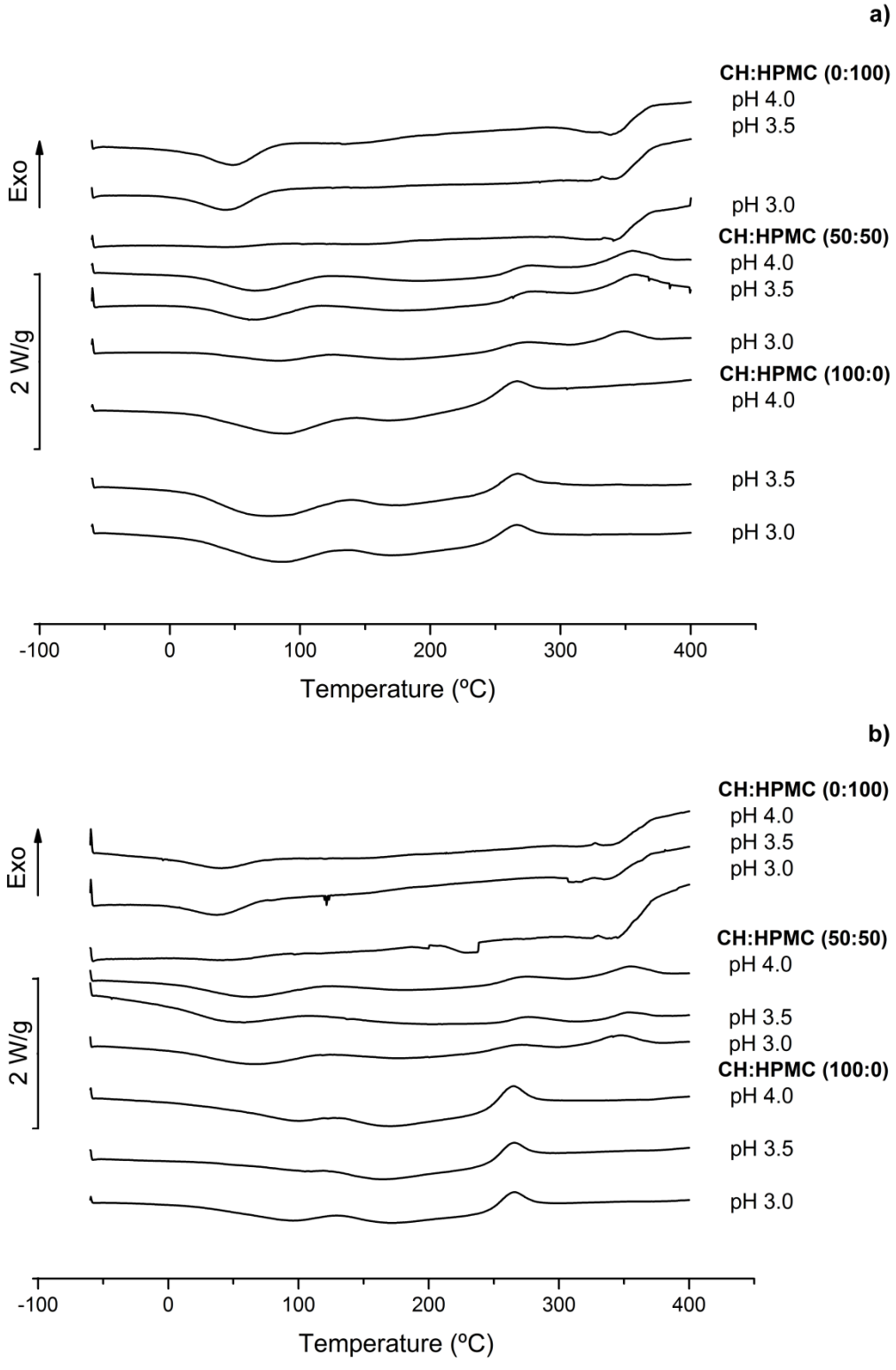

Figure 3. DSC thermograms of the CH:HPMC (X:Y), pH 3-4 hydrogel films, obtained by a) FT and b) SC, for the polymeric compositions 0:100, 50:50 and 100:0.

Or

Figure 3. DSC thermograms of the CH:HPMC (0:100, 50:50 and 100:0), pH 3-4 hydrogel films, obtained by a) FT and b) SC techniques.

Table 1: DSC thermal events of CH:HPMC (X:Y), pH 4, FT and SC hydrogel films.

CH:HPMC	Endothermic peak I		Endothermic peak II		Endothermic peak III		Exothermic peak	
FT	**T_{onset} ± 0.02 (ºC)**	**ΔH (J/g)**	**T_{onset} ± 0.02 (ºC)**	**ΔH (J/g)**	**T_{onset} ± 0.02 (ºC)**	**ΔH (J/g)**	**T_{onset} ± 0.02 (ºC)**	**ΔH (J/g)**
0:100	-12.63	-149.12	*	*	299.93	*	-	-
10:90	0.34	-92.14	-	-	-	-	335.44	*
20:80	-1.79	-73,74	119.02	-29.05	-	-	338.75	*
30:70	16.24	-55.40	144.77	*	-	-	318.04	60.37
40:60	24.72	-57.87	136.09	*	-	-	316.79	47.81
50:50	13.58	-122.10	139.61	*	-	-	320.91	55.32
60:40	23.02	-44.29	139.41	*	-	-	317.22	51.77
70:30	14.40	-79.39	136.53	*	-	-	302.21	42.86
80:20	6.59	-122.13	133.11	*	-	-	*	*
90:10	4.84	-56.56	144.14	*	-	-	*	*
100:0	12.49	-166.61	146.45	*	-	-	*	*
SC								
0:100	-15.82	-99.33	-	-	296.40	-7.21	-	-
10:90	9.06	-53.23	*	*	*	*	*	*
20:80	11.97	-143.20	-	-	-	-	321.40	*
30:70	5.34	-153.07	-	-	-	-	*	*
40:60	$-22.95x10^{-3}$	-104.84	122.44	*	-	-	316.19	*
50:50	-12.70	-144.38	130.58	-124.19	-	-	*	*

60:40	11.98	-158.49	123.19	-194.58	-	-	297.30	
70:30	0.87	-135.00	142.62	*	-	-	297.47	54.48
80:20	-	-	124.17	-89.52	-	-	300.38	*
90:10	-20.14	*	*	*	-	-	*	*
100:0	-1.64	*	*	*	-	-	*	*

(*) This parameter was impossible to be determined.

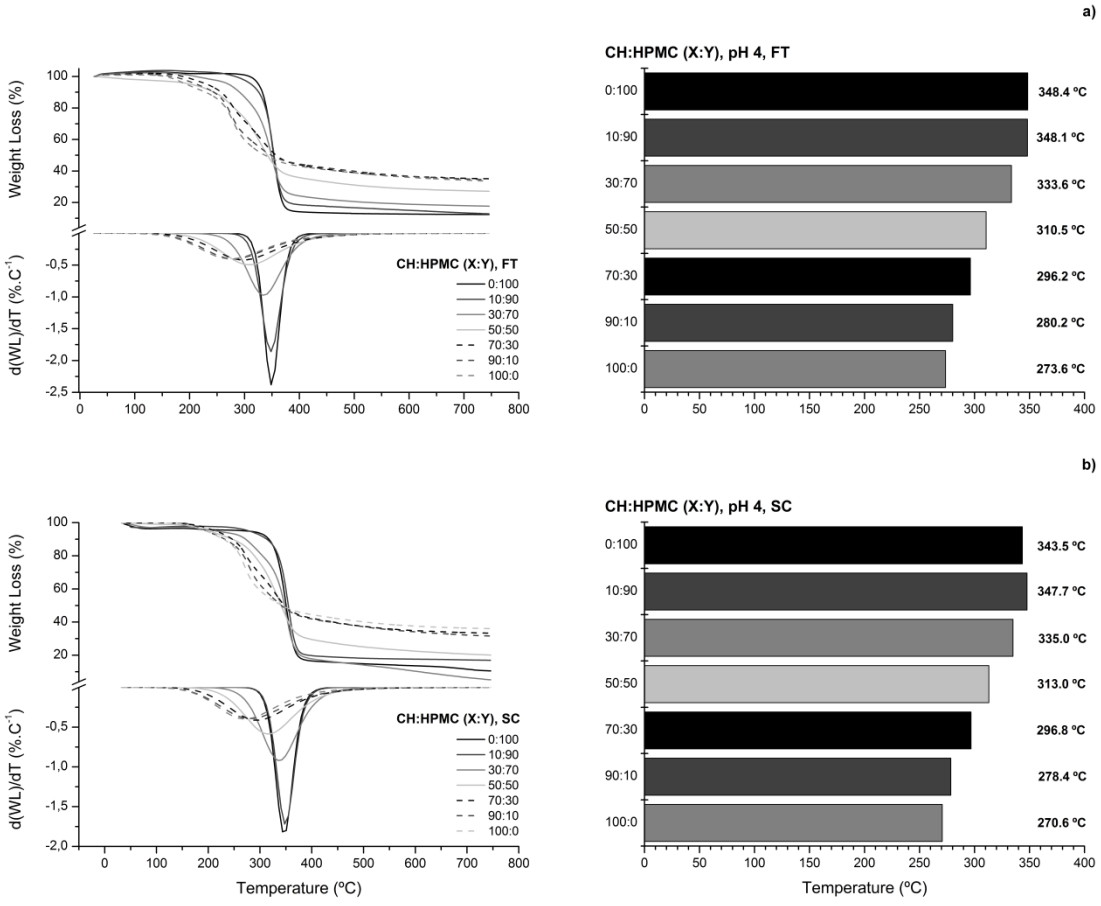

Figure 4. TGA and DTG thermograms of the CH:HPMC (X:Y), pH4 hydrogel films, for the compositions 100:0, 10:90, 30:70, 50:50, 70:30, 90:10 and 100:0, attained by a) FT and b) SC. These assays were performed in a Shimadzu TGA-50 equipment, at a temperature range between 30 and 750ºC and a heating rate of 10ºC.min^{-1}, under nitrogen purge (50 mL/min).

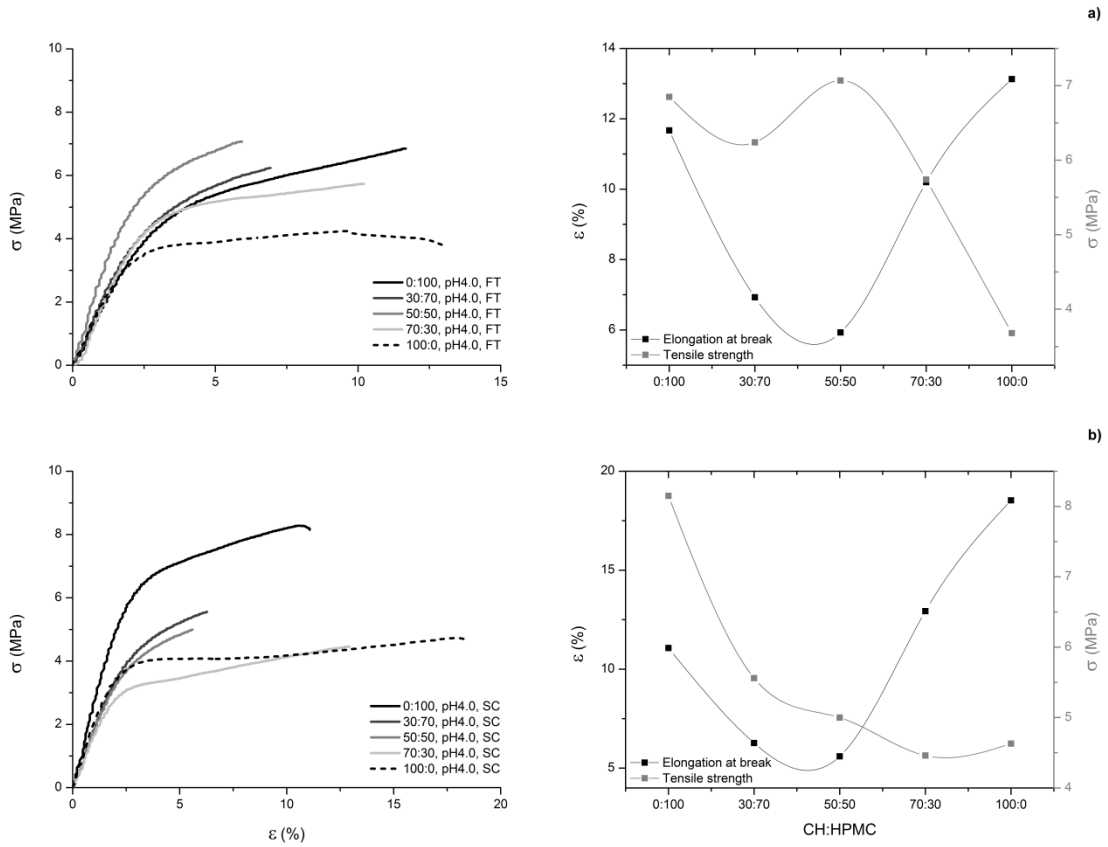

Figure 5. Stress-strain curves (tensile strength (σ) *versus* elongation (ε)) and composition influence on tensile strength and elongation at break for the CH:HPMC hydrogel films, prepared by a) FT and b) SC techniques. These assays were performed in a Linkam TST350 tensile stress testing system with a load cell of …Newtons (N), at room temperature. At least three measurements of tensile strength and elongation at break were recorded for each membrane analysed and a mean value was calculated.

a)

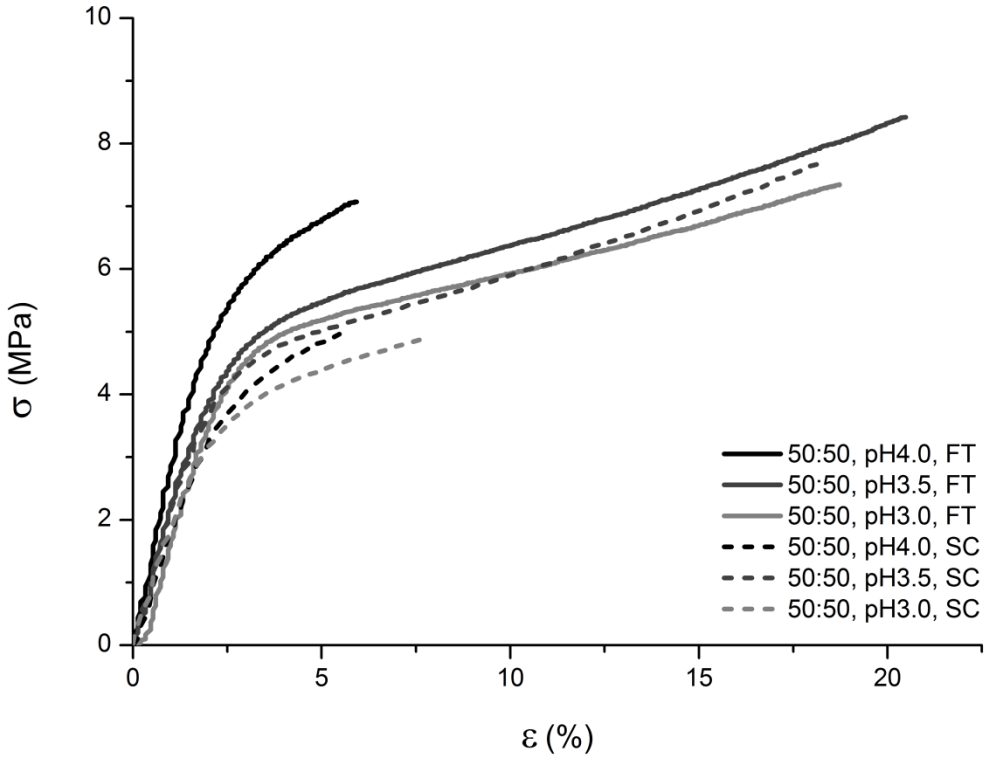
σ (MPa)
ε (%)
50:50, pH4.0, FT
50:50, pH3.5, FT
50:50, pH3.0, FT
50:50, pH4.0, SC
50:50, pH3.5, SC
50:50, pH3.0, SC

b)

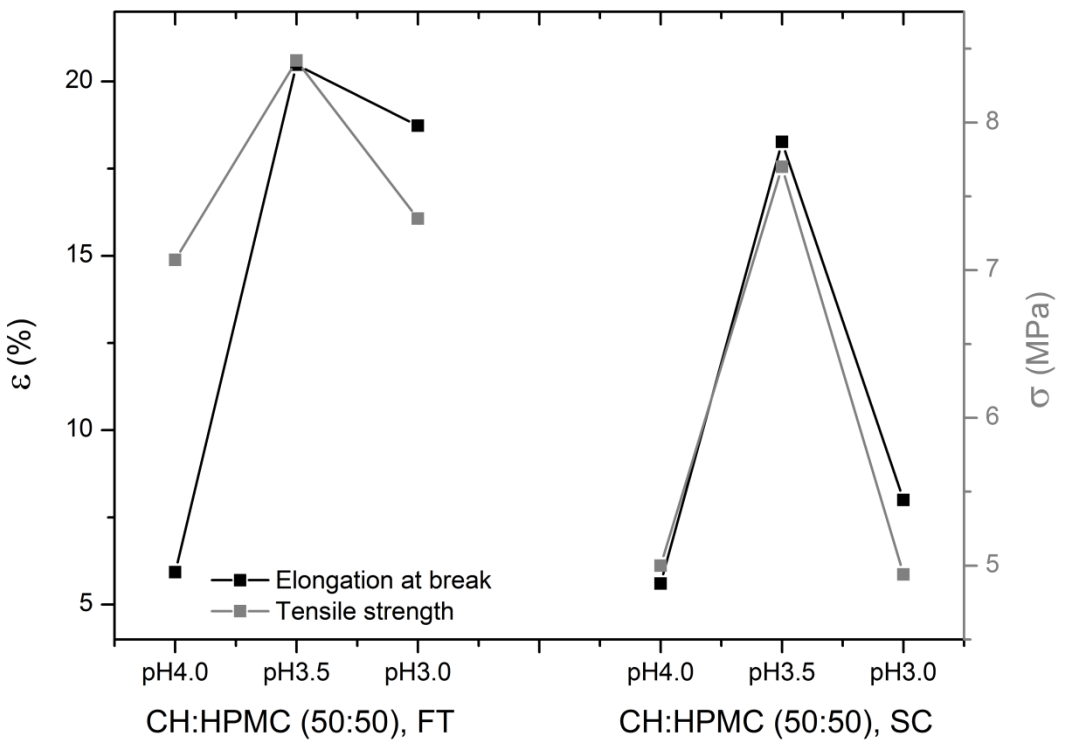
ε (%)
σ (MPa)
Elongation at break
Tensile strength
pH4.0
pH3.5
pH3.0
CH:HPMC (50:50), FT
CH:HPMC (50:50), SC

Figure 6. Stress-strain curves and composition influence on tensile strength (σ) and elongation (ε) at break of the CH:HPMC (50:50), FT and SC membranes, prepared at different pH values (3.0, 3.5 and 4.0).

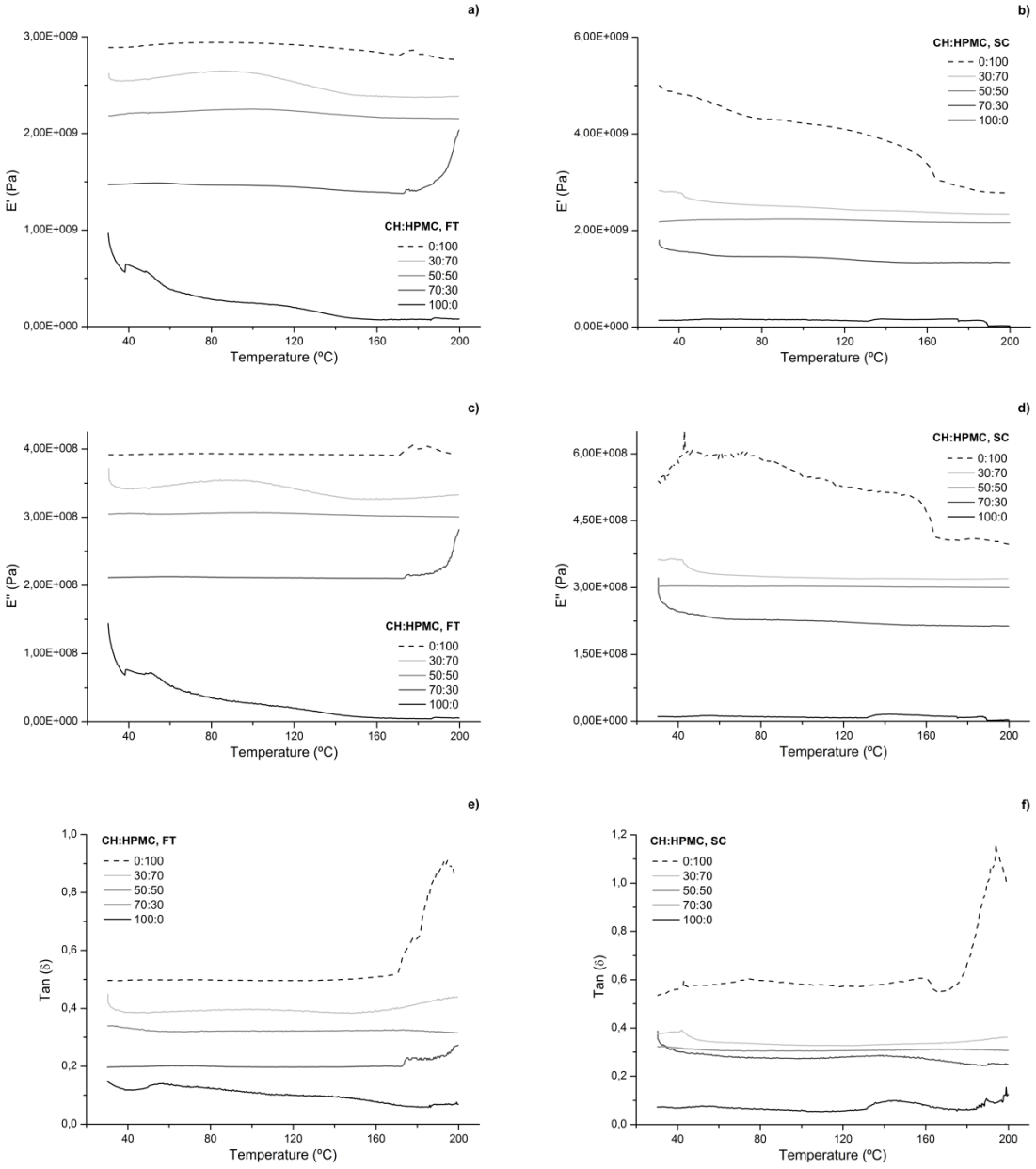

Figure 7. Rheological behaviour of CH:HPMC (X:Y), pH 4 hydrogel films, prepared by a, c, e) FT and b, d, f) SC techniques. These assays were performed in a Seiko DMS210 instrument, from 30 up to 200 ºC, at a heating rate of 2 ºC.min^{-1} and a frequency of 1 Hz, in tensile mode.

a)

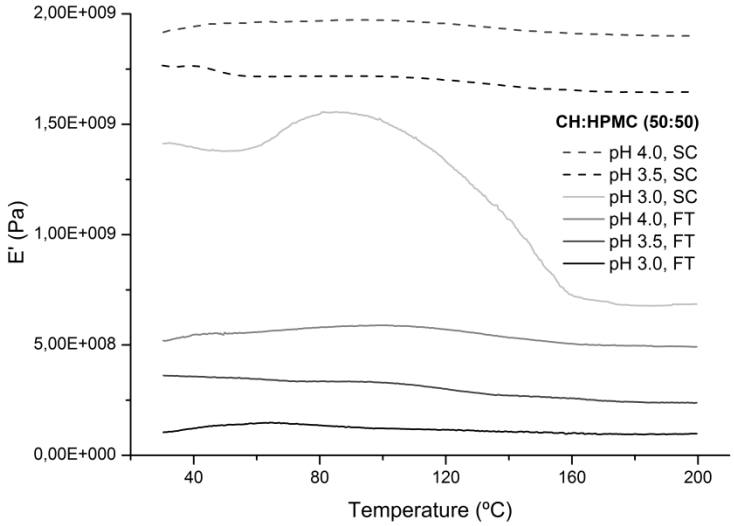
2,00E+009
1,50E+009
1,00E+009
5,00E+008
0,00E+000
E' (Pa)
40
80
120
160
200
Temperature (ºC)
CH:HPMC (50:50)
pH 4.0, SC
pH 3.5, SC
pH 3.0, SC
pH 4.0, FT
pH 3.5, FT
pH 3.0, FT

b)

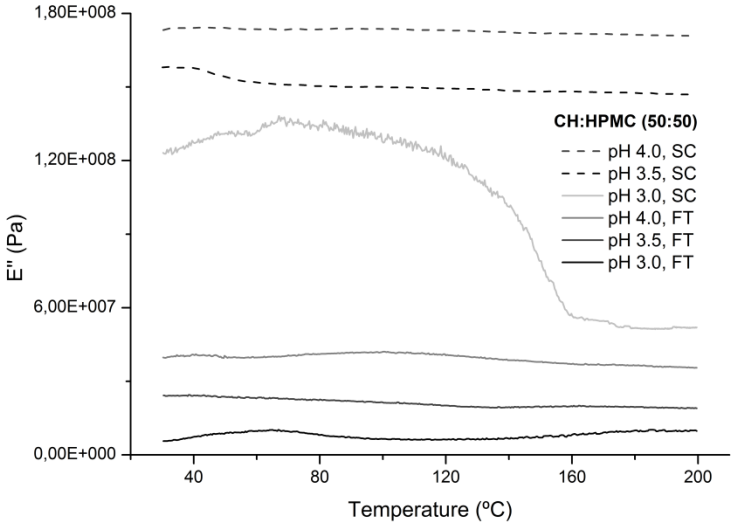
1,80E+008
1,20E+008
6,00E+007
0,00E+000
E'' (Pa)
40
80
120
160
200
Temperature (ºC)
CH:HPMC (50:50)
pH 4.0, SC
pH 3.5, SC
pH 3.0, SC
pH 4.0, FT
pH 3.5, FT
pH 3.0, FT

c)

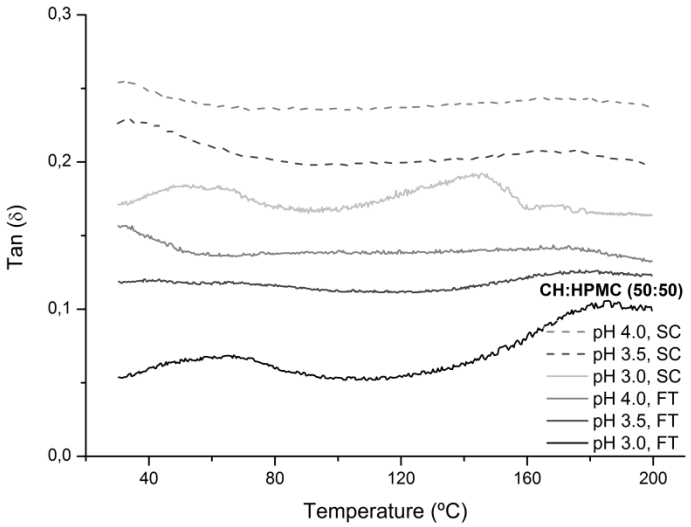
0,3
0,2
0,1
0,0
Tan (δ)
40
80
120
160
200
Temperature (ºC)
CH:HPMC (50:50)
pH 4.0, SC
pH 3.5, SC
pH 3.0, SC
pH 4.0, FT
pH 3.5, FT
pH 3.0, FT

Figure 8. Dynamic mechanical spectra of CH:HPMC (50:50), pH 3-4 hydrogel films, attained by FT and SC process.

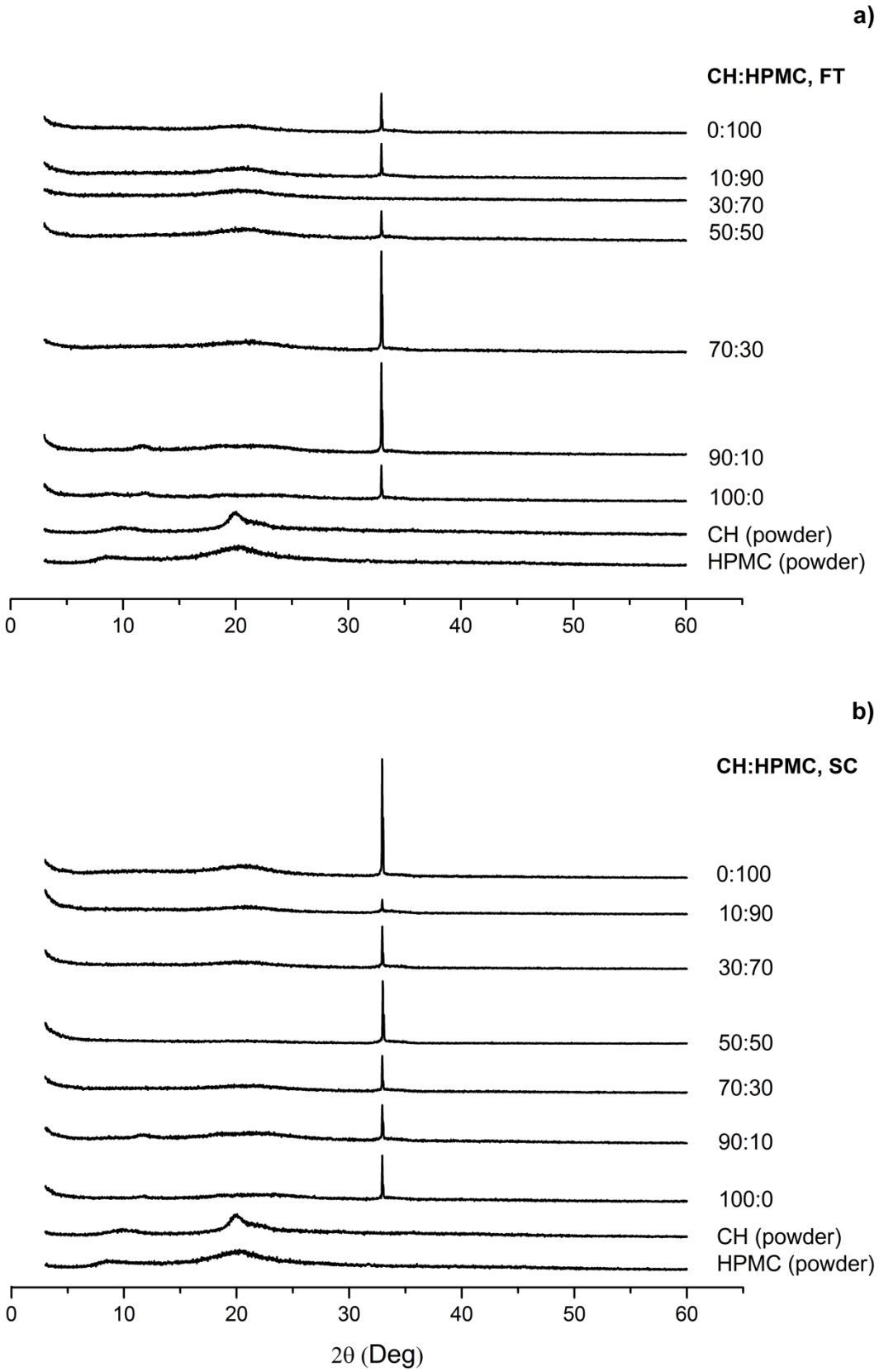
a)
CH:HPMC, FT
0:100
10:90
30:70
50:50
70:30
90:10
100:0
CH (powder)
HPMC (powder)
0
10
20
30
40
50
60
b)
CH:HPMC, SC
0:100
10:90
30:70
50:50
70:30
90:10
100:0
CH (powder)
HPMC (powder)
0
10
20
30
40
50
60
2θ (Deg)

Figure 9. X-ray diffraction patterns of CH:HPMC (X:Y), pH 4.0 a) FT and b) SC hydrogel films and CH and HPMC polymers. These assays were performed in a PANalytical X'Pert Pro instrument with Cu Kα (λ=1,541 Å) radiation, over a range of diffraction angle (2θ) from 3 to 60º.